CHAPTER VII

THE ROLE OF FERROFLUID ON SURFACE SMOOTHNESS OF BACTERIAL CELLULOSE NANOCOMPOSITE DISPLAY

7.1 Abstract

Ferrofluid solution was successfully synthesized by wet chemical route. X-ray diffraction and transmission electron microscope were employed to investigate the crystal phase structure and particle size diameter, respectively. After synthesis, the average diameter of solid particle size is ~ 30 nm. Furthermore, the ferrofluid solution was used as nano-abrasion media for surface smoothness enhancement of bacterial cellulose nanocomposite. Atomic force microscope revealed that significant enhancement of surface smoothness reach 5 nm, suggesting that bacterial cellulose nanocomposite substrate can be excellent candidate for organic light emitting diode.

7.2 Introduction

The study on ferrofluid properties and application has been evident in the past decade [2, 4, 9, 81, 158-162]. Ferrofluid, a colloidal mixture consisted of magnetic nanoparticle, disperses in a carrier liquid such as water or organic solvent. It becomes polarized in the presence of a magnetic field. In general, the diameter of magnetic particle in this fluid is about 30 nm and a surfactant is used as stabilizer. Ferrofluid solution can flow. Its rheological properties can be controlled by applying the magnetic field.

Interest is, therefore, achievement of this concept can easily lead to biomedical device [157, 163], electronic sensor device [164, 165] as well as controllable device of agricultural product application [166]. Among the device applications, electronic device namely "organic light emitting diode" is a versatile platform system that has attracted worldwide attention [1]. Organic light emitting diode has been traditionally fabricated on glass sheet. The use of polymer substrates has been expected as potential candidate in replacing the rigid and brittle glass

substrate in order to achieve flexible feature. In order to combine the flexible feature and "Green concept" [23-25] which was defined as the design of product and process that minimize the use and the generation of hazardous materials, in this work, the use of cellulose nanocomposite as flexible display is reported.

By the way, we have previously reported the successful fabrication of flexible substrate for organic light emitting diode (OLED) based on cellulose nanocomposite [167]. The nanocellulose prepared from both pulp fiber [9, 168] and bacterial cellulose "*Acetobacter Xylinum*" [10] provided us as excellent candidate for OLED device substrate. Up to the present time, the property of this substrate was continuously developed by Si-O deposition. The use of this nanolayer deposited by plasma enhanced chemical vapor deposition (PECVD) can protect the substrate from surrounding water vapor and enhanced the surface smoothness [169]. Therefore, the device lifetime can be extended. However, it has been suggested that, for the effective OLED, the surface roughness of the substrate should be kept lower than 5 nm [8]. In order to overcome this issue, several polishing techniques have been investigated. The critical challenge lies in the use of ferrofluid that offers more smoothness in surface.

Therefore, in this research work, we studied the preparation of ferrofluid for cellulose nanocomposite substrate. The preparation and characterization of bacterial cellulose nanocomposite have been discussed elsewhere [167]. The main motivation for use ferrofluid is to use as abrasion media nanoparticle in processing step in order to reduce the surface roughness of flexible display substrate.

7.3 Materials, Methods And Instruments

7.3.1 Materials

Ferrous chloride 4-hydrates ($FeCl_2$. $4H_2O$) (purity >99.9%), Ferrous chloride 6-hydrates ($FeCl_3.6H_2O$) and Al_2O_3 were purchased from J. T. Baker Chemical Co, Phillipsburg, Canada. Ammonia (NH_4OH), Iron particle and castor oil were purchased from Sigma Aldrich, Canada. All of these products were analytical grade and used as received without further purification.

7.3.2 Methods

- Bacterial Cellulose Nanocomposite Preparation

To fabricate the nanocomposite, the bacterial cellulose sheet was first prepared from bacterial cellulose suspension. The water was removed from the suspension through filtration with a Buchner funnel fitted with Polyterafluoroethylene membrane filter (0.1 μm mesh, 90 mm diameter), which was connected to a Buchner flask and a vacuum pump. The volume of the bacterial cellulose suspension was adjusted to achieve a bacterial cellulose disc with the dried weight of 0.25 g. The filtration was continued until the wet sheet of bacterial cellulose was formed. The wet sheet was then dried between two Polyterafluoroethylene membranes under the applied pressure of 58 psi, following the paper hand sheet formation standard SCAN C 26:76. The dried bacterial cellulose sheet was then impregnated with PU resin and cured under UV at 25 mW/cm^2 for 3 minutes. As a reference, the neat PU based resin sheet was also fabricated in similar manner. All samples had the thickness of 0.3 mm. All experiments involving the resin were conducted in dark room as the resin was sensitive to light. The fiber content of the nanocomposite was 10 - 50 wt %.

Additional information of nanocomposite preparation and characterization has been reported in our previous article [167].

- Synthesis Of ferrofluid

The co-precipitation method was used to synthesize ferrofluid. The synthetic process from the salt solution occurred in accordance with the reaction:

$$FeCl_2.\ 4H_2O + 2FeCl_3.6H_2O + 8NH_4OH \rightarrow Fe_3O_4 + 8NH_4Cl + 20H_2O$$

A solution of $FeCl_3.6H_2O$ (0.3 M) and $FeCl_2.\ 4H_2O$ (0.3) mixed in a molar ratio of 2:1 was prepared. An ammonia aqueous solution of 20 ml was then added with vigorous stirring using mechanical stirrer. The reaction was conducted for 5 hours. A black precipitation was obtained. After that castor oil of 20 ml was added and intensely stirred at 70°C for 1 hour. The precipitation was filter and washed with deionized water several times. The ferrofluid solution was centrifuged and kept in desiccators in order to prevent moisture sensitive problem.

- Preparation Of Magnetic Compound Fluid (MCF)

The formulation of magnetic compound fluid (MCF) can be prepared in Table 7.1.

Table 7.1 Formulation of magnetic compound fluid (MCF)

Condition of Magnetic compound fluid	Al_2O_3 (%wt)	Iron (%wt)	Ferrofluid (%wt)
(A)	12	41	47
(B)	6	20	74

Magnetic compound fluid consists of ferrofluid, Al_2O_3 and iron particle. The diameter of particle size of Al_2O_3 and iron particle was 0.3 and 1 μm, respectively. They were used to be well responded with magnetic field. This might lead the excellence in compatibility with synthetic ferrofluid solution. Also, the use of these can be controlled the viscosity of magnetic compound fluid.

Therefore, magnetic compound fluid can be distributed the shear force from iron to bacterial cellulose nanocomposite in polishing step.

- Abrasion Processing Technique Of Magnetic Compound Fluid

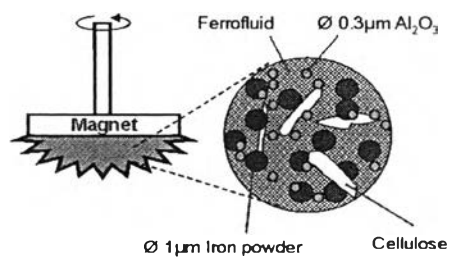

Figure 7.1 Schematic drawing of processing principle

Figure 7.1 represents the abrasion processing technique. Magnetic compound fluid polishing liquid in nano-precision surface of cellulose nanocomposite was successfully developed. In general, it is commonly produced by the mixture between iron nanoparticle and solvent. The use of magnetic compound fluid as nano-precision surface polishing can easily lead to enhance the surface smoothness of cellulose nanocomposite. Here, a disc-shaped permanent magnet is attached as the holder and located above the sample; magnetic compound fluid is put into the gap between the magnet and sample. Magnetic nanoparticle clusters are formed along the magnetic field immediately. When the magnet holder is rotated around its axis, the magnet follows the rotation of holder and the clusters are rotated around the magnet axis due to the magnetic force, hence carry the abrasive particle to generate a relative speed between the abrasive particles and the sample. As a result, the surface of sample is smoothened by nano-cutting action of abrasive particle.

7.3.3 Instruments

- X-ray Diffraction (XRD)

After solid particle was casted on glass slide, process of heat treatment was conducted for solvent removal; solid particle can be then obtained. The film was identified for crystal structure by XRD (Phillips P.W. 1830 diffractrometer) using nickel-filtered CuKα radiation. Diffraction patterns were recorded over a range of 2θ angles from 20-70°. The consistent of result was compared with literature [158, 165, 166].

- Transmission Electron Microscope (TEM)

The solid particle size of ferrofluid solution was investigated by TEM, Hitachi H-7000. The solution was suspended in methanol and dropped on a molybdenum grid. After that, the grid was dried at 50°C for methanol evaporation and kept into the TEM chamber. The image thus obtained was processed with computer for identification of the domains in which certain lattice fringes appear. For this propose, TEM image was captured under 50000X and 100000X magnification. The acceleration voltage of electron beam was set at 100 keV.

- Rheometer

The rheological properties of the magnetic compound fluid were measured with RH2000 Rheometer, The shear rate range and applied pressure were set between 0-10 s^{-1} and 0.1 Pa, respectively. The measurements were repeated five times and the statistical average data was used to plot curve.

- Atomic Force Microscope (AFM)

AFM was performed with a Digital Instruments Nanoscope III Scanning Probe Microscope (Digital Instruments, CA, USA) in ambient conditions (22°C, 45-55% relative humidity) over areas of 5 μm x 5 μm and 1 μm * 1 μm. The instrument was equipped with silicon nitride tip and operated in the lateral contact mode. The measurements were repeated five times for comparable topological analysis.

7.4) Results And Discussion

- Synthesis and characterization of ferrofluid

The ferrofluid was successfully synthesized and obtained as a black viscous fluid. After castor oil removal by centrifugation, magnetic nanoparticle was precipitated. It is commonly known that magnetic nanoparticle is not stable, especially under moisture condition. The nanoparticle can be oxidized and therefore lose magnetism gradually, which is consequently detrimental to application. To maintain the magnetic nanoparticle stability, the synthesized product was stored in desiccators before usage.

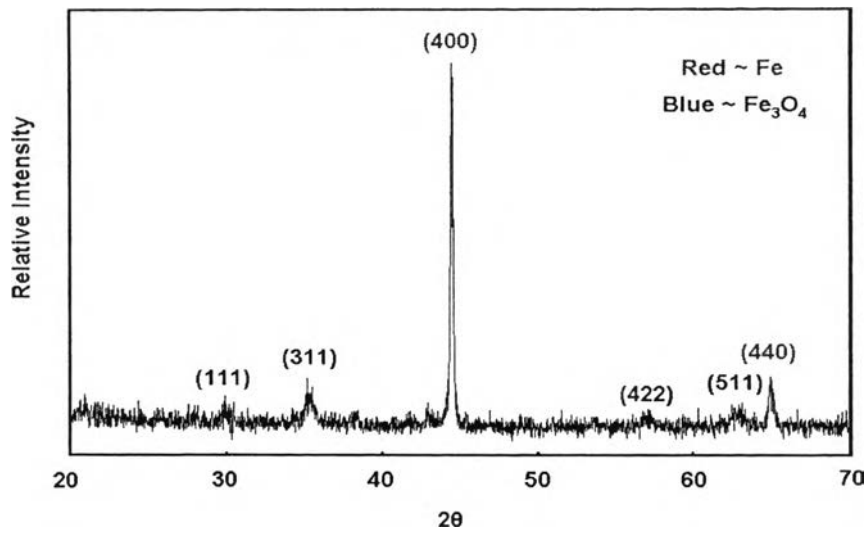

Figure 7.2 XRD pattern of ferrofluid nanoparticle in solid state

Figure 7.2 exhibits the X-ray powder diffraction of ferrofluid in solid state. After precipitation, solid nanoparticle was casted on glass slide and subsequently dried over night. It can be determined that ferrofluid nanoparticle is well crystallized. However, it can be observed that the peak presents two phases. The presence of Fe phase and Fe_3O_4 phase was indicated. However, we believe that the quantity of Fe phase is higher than Fe_3O_4 phase due to the strong intensity of XRD line (400), corresponding to Fe phase. The first phase can be remarkably observed at 44° and 65° corresponding to the face-centered cubic structure of Fe crystal planes (400) and (440), respectively. While, the second phase can also be remarkably observed at 30°, 36°, 58° and 63° corresponding to the face-centered cubic structure of Fe_3O_4 crystal planes (111), (311), (422) and (511), respectively.

In addition, the particle sizes of ferrofluid particle can be calculated from peak of XRD spectra based on the Scherrer 's equation:

$$D= k\lambda/(\beta\cos\theta)$$

where D is the average particle size, k is a constant taken as 0.9 for calculation, β is the full width at half maximum (FWHM) in radians, λ is the wavelength of the X-ray, and θ is the diffraction angle [170]. From the Scherrer 's equation, the synthesized ferrofluid has been calculated to be roughly 30 nm at (400) peak, respectively. This is close to the value deduced from TEM image.

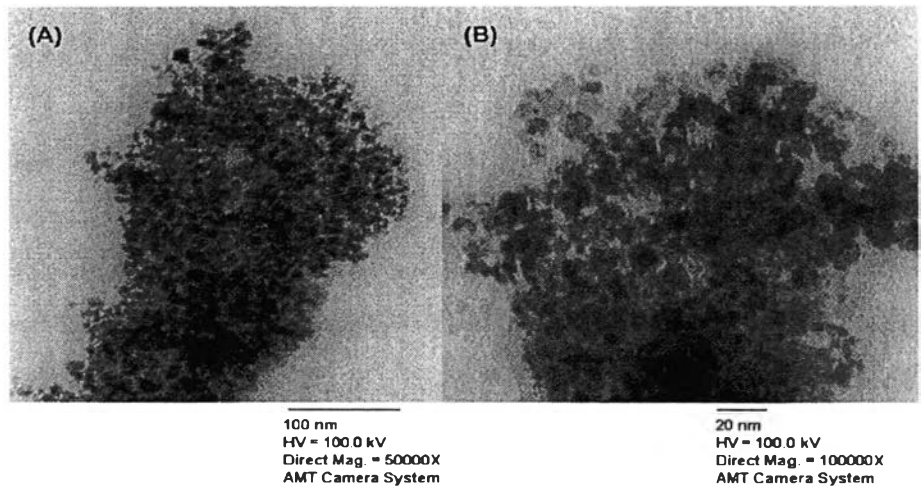

Figure 7.3 TEM investigation of ferrofluid solid nanoparticle
(A) magnification 50000X (B) magnification 100000X

TEM microscopy was used to determine the particle size and particle size distribution of magnetic nanoparticle in aqueous solution without magnetic field. Figure 7.3A and 7.3B represent particle size of magnetic nanoparticle with 50000X and 100000X of magnification, respectively. They exhibit the irregular shapes of the magnetic nanoparticle. As exhibited in Figure 7.4, the mean average particle size and standard deviation were roughly estimated to be 30.6 and 9.8 nm, respectively. In the order of magnitude the theoretical results are in agreement with the result of the XRD measurement, presented in Figure 7.2. However, the magnetic nanoparticle exhibited the cluster form having raspberry-like structure in the absence of magnetic field.

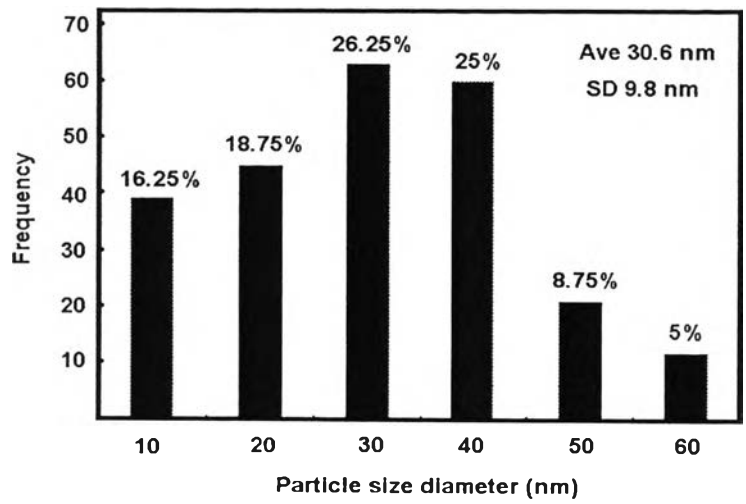

Figure 7.4 Histogram of magnetic nanoparticle in aqueous solution

- Study on rheological properties of ferrofluid

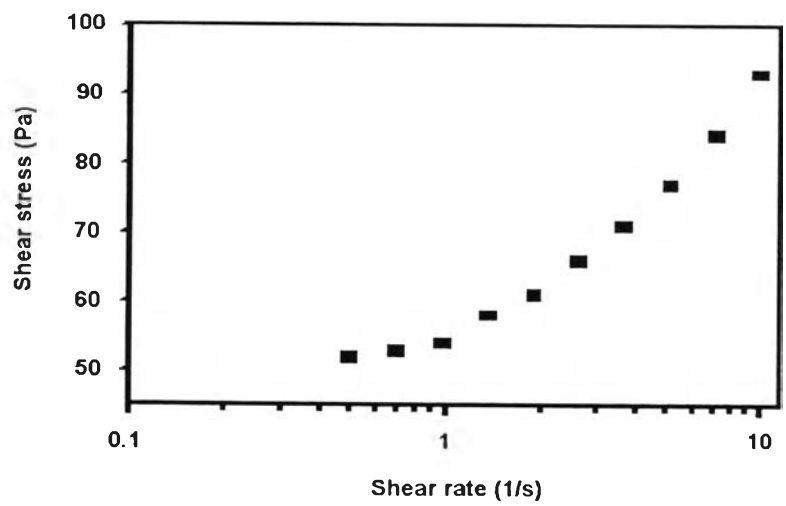

Figure 7.5 Shear stress versus shear rate of ferrofluid

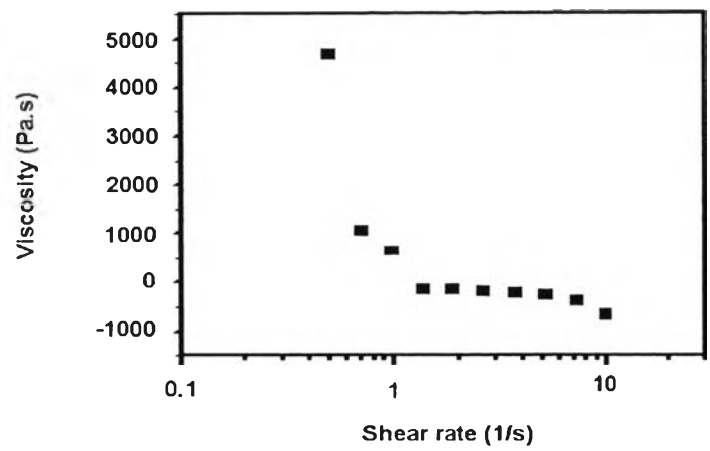

Figure 7.6 Shear thinning behavior of the ferrofluid

Figure 7.5 represents the curve of shear stress versus shear rate. It can be noted that the existence of yield stress is due to the interaction forces of fluid nanoparticles as they initially resist fluid motion. Moreover, the rheological properties can be investigated in Figure 7.6 that, the viscosity of ferrofluid decreases with increasing shear rate, which can be indicated as "shear thinning behavior". It can be explained that when the applied shear rate increases, the nanoparticles begin to arrange their orientation in the shear direction. Furthermore, increasing shear rate destroys the initial bonds existing among the nanoparticles, and as a subsequence, the viscosity of fluid decreases.

- Surface analysis of bacterial cellulose nanocomposite

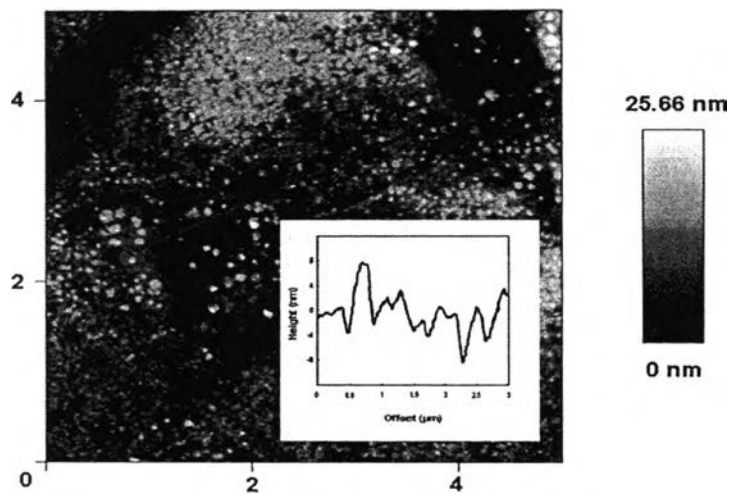

Figure 7.7 Top view AFM image of polishing condition A

Figure 7.7 exhibits AFM image taken with lateral contact mode of sample polished with ferrofluid condition A. In this research work, five AFM images were taken at different areas on the sample, all of which revealed comparable topologies. The AFM scan size (5 μm * 5 μm) implied the uniformity of the surface smoothness. According to our previous work, Ummartyotin et al also reported the smoothness of surface of flexible substrate as 81.39 nm [169]. After polishing by ferrofluid, the sheet roughness reduced to 25.66 nm as scratches on surface were completely removed. In addition, part of image, indicated as blue line, was sampled from the relatively smooth area for the Fourier transformed pattern analysis [171] – an alternative analysis proposed to facilitate the assessment of 2D surface morphology. This technique related a statistical analysis to derive statistical parameters which are correlated with surface roughness. In this experiment, the length of the blue line is 3.12 μm and the average surface roughness is ~ 5 nm. Its roughness was equal the specification of flexible OLED substrate, as suggested by Choi et al [8].

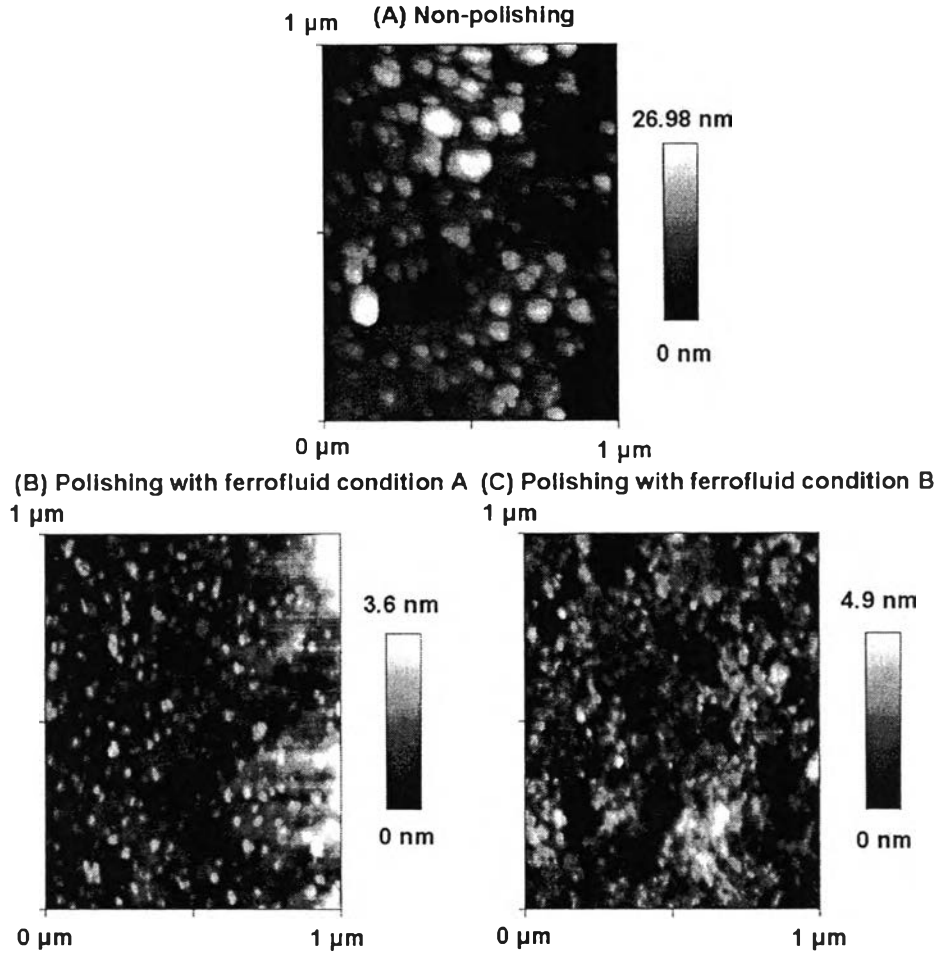

Figure 7.8 Top view AFM image of (A) Non-polishing (B) Polishing with ferrofluid condition A (C) Polishing with ferrofluid condition B

Figure 7.8 also illustrates AFM image taken with lateral contact mode. In this work, the AFM scan size (1 µm * 1 µm) were consequently taken. The representation of Figure 6.7 is to use to give explanation of surface analysis in smaller area, which concerned with 2D analysis in Figure 7.7. The roughness of surface was ~ 5 nm. After polishing by ferrofluid, the roughness was significantly reduced from 26.98 nm to 3.6 and 4.9 nm of both different composition of ferrofluid. It is important to note that the use of ferrofluid in polishing step lead us to achieve the smoothness of surface less than 5 nm. Our polished surface reach the specification of OLED substrate, cited by Choi et al [8].

7.5 Conclusion

Ferrofluid solution was successfully synthesized by wet chemical synthetic route. It was used as nano-abrasion media for polishing with cellulose nanocomposite substrate. The roughness of surface was less than 5 nm. Therefore, this experiment can lead us to further develop and scale up flexible substrate of organic light emitting diode (OLED) industry.

7.6 Acknowledgement

The authors would like to thank ABIP, NSERC Manufacturing Network and CG Tower for their financial supports. AFM investigation by Mr. Calvin Cheng in Prof. Cynthia Goh lab, Institute of Optical Science, University of Toronto is gratefully acknowledged. SU would like to acknowledge the scholarship from the Center of Excellence for Petroleum, Petrochemicals and Advanced Materials, Chulalongkorn University.

7.7 References

D. Borin, A. Zubarev, et al., Ferrofluid with clustered iron nanoparticles: slow relaxation of rheological properties under joint action of shear flow and magnetic field, Journal of Magnetism and Magnetic Materials 323 (2011) 1273–1277.

A. Bozhko, T. Tynjala, Influence of gravitational sedimentation of magnetic particles on ferrofluid convection in experiments and numerical simulations, Journal of Magnetism and Magnetic Materials 289 (2005) 281–284.

M.C. Choi, Y. Kim, et al., Polymers for flexible displays: from materials selection to device application, Progress in Polymer Science 33 (2008) 581–630.

R. Ganguly, A.P. Gaind, et al., Analyzing ferrofluid transport for magnetic drug

targeting, Journal of Magnetism and Magnetic Materials 289 (2005) 331–334.

E. Ghasemi, A. Mirhabibi, et al., Synthesis and rheological properties of an iron oxide ferrofluid, Journal of Magnetism and Magnetic Materials 320 (2008) 2635–2639.

B. Greffroy, P. Le Roy, et al., Review: organic light emitting diode (OLED) technology: materials, devices and display technologies'', Polymer International 55 (2006) 572–582.

A. Halbreich, J. Roger, et al., Biomedical applications of magnetite ferrofluid, Biochimie 80 (1998) 379–390.

H. Hartshorne, C.J. Backhouse, et al., Ferrofluid-based microchip pump and valve, Sensors and Actuators B: Chemical 99 (2004) 592–600.

J. Juntaro, Environmentally friendly hierarchical composites, Ph.D. Thesis, Department of Chemical Engineering and Chemical Technology London, University of London (2009).

M.M. Kirchhoff, Promoting sustainability through green chemistry, Resources, Conservation and Recycling 44 (2005) 237–243.

A.A. Kubasov, Electromotive force generation due to ferrofluid motion, Journal of Magnetism and Magnetic Materials 173 (1997) 15–19.

J.B. Manley, P.T. Anastas, et al., Frontiers in green chemistry: meeting the grand challenges for sustainability in R&D and manufacturing, Journal of Cleaner Production 16 (2008) 743–750.

L. Martinez, F. Cecelja, et al., A novel magneto-optic ferrofluid material for sensors applications, Sensors and Actuators A: Physical 123–124 (2005) 438–

443.

S. Masoud Hosseini, A. Fazlali, et al., Rheological properties of a Fe2O3 paraffinbased ferrofluid, Journal of Magnetism and Magnetic Materials 322 (2010) 3792–3796.

M. Pinho, B. Brouard, et al., Investigation into ferrofluid magnetoviscous effects under an oscillating shear flow, Journal of Magnetism and Magnetic Materials 323 (2011) 2386–2390.

M. Racuciu, D.E. Creanga, Influence of water-based ferrofluid upon chlorophylls in cereals, Journal of Magnetism and Magnetic Materials 311 (2007) 291–294.

M.M. Sain, A. Bhatnagar, Manufacturing process of cellulose nanofibers from renewable feed stocks, US 0146701 (2008).

Z.G. Shi, Y. Zhang, et al., Ferrofluid-based liquid-phase microextraction, Journal of Chromatography A 1217 (2010) 7311–7315.

C. Suryanarayana, M. Grant Norton, X-ray diffraction: A practical approach, Plenum Press, New York, 1998.

M. Tomita, T. Hashimoto, et al., Improvement and application of the fouriertransformed pattern from a small area of high resolution electron microscope images, Ultramicroscopy 16 (1985) 9–18.

S. Ummartyotin, J. Juntaro, et al., Development of transparent bacterial cellulose nanocomposite film as substrate for flexible organic light emitting diode (OLED) display, Industrial Crops and Products 35 (2012) 92–97.

S. Ummartyotin, J. Juntaro, et al., Si–O barrier technology for bacterial cellulose

nanocomposite flexible displays, Carbohydrate Polymers 86 (2011) 337–342.

J.C. Warner, A.S. Cannon, et al., Green chemistry, Environmental Impact Assessment Review 24 (2004) 775–799.

C. Wu, Production and characterization of optically transparent nanocomposite film, Faculty of Forestry, Toronto, University of Toronto.

Y. Wu, T. Sato, et al., The detailed performance of MCF polishing liquid in nanoprecision surface treatment of acrylic resin, Advanced Materials Research 76–78 (2009) 331–336.

Y. Wu, T. Sato, et al., MCF (Magnetic Compound Fluid) polishing process for free-formed resin device using robotic arm, International conference of advances in materials and processing technologies (AMPT2010)